

This discussion paper is/has been under review for the journal The Cryosphere (TC).  
Please refer to the corresponding final paper in TC if available.

# Recent summer Arctic atmospheric circulation anomalies in a historical perspective

**A. Belleflamme, X. Fettweis, and M. Erpicum**

Laboratory of Climatology, Department of Geography, University of Liège, Allée du 6 Août, 2,  
4000 Liège, Belgium

Received: 18 July 2014 – Accepted: 18 August 2014 – Published: 10 September 2014

Correspondence to: A. Belleflamme (a.belleflamme@ulg.ac.be)

Published by Copernicus Publications on behalf of the European Geosciences Union.

**TCD**  
8, 4823–4847, 2014

Recent summer  
Arctic circulation  
anomalies in  
a historical  
perspective

A. Belleflamme et al.

Title Page

Abstract

Introduction

Conclusions

References

Tables

Figures

◀

▶

Back

Close

Full Screen / Esc

Printer-friendly Version

Interactive Discussion



## Abstract

A significant increase in the summertime occurrence of a high pressure area over the Beaufort Sea and Greenland has been observed from the beginning of the 2000's, and particularly between 2007 and 2012. These circulation anomalies are likely partly responsible for the enhanced Greenland ice sheet melt as well as the Arctic sea ice loss observed since 2007. Therefore, it is interesting to analyse whether similar conditions might have happened since the late 19th century over the Arctic region. We have used an atmospheric circulation type classification based on daily mean sea level pressure and 500 hPa geopotential height data from four reanalysis datasets (ERA-Interim, ERA-40, NCEP/NCAR, and 20CRv2) to put the recent circulation anomalies in perspective with the atmospheric circulation variability since 1871. We found that circulation conditions similar to 2007–2012 have occurred in the past, despite a higher uncertainty of the reconstructed circulation before 1940. But the recent anomalies largely exceed the interannual variability of the atmospheric circulation of the Arctic region. These circulation anomalies are linked with the North Atlantic Oscillation suggesting that they are not limited to the Arctic. Finally, they favour summertime Arctic sea ice loss.

## 1 Introduction

Over the last years, and particularly since 2007, significant atmospheric circulation anomalies have been observed over different parts of the Arctic. Based on 500 hPa geopotential height (Z500), Fettweis et al. (2013) reported a doubled frequency of summertime anticyclones centred over Greenland, representing an increased frequency of negative NAO (North Atlantic Oscillation) conditions. This circulation anomaly impacts the climate of a major part of the Arctic region by favouring warm southerly air advection over Greenland and the Canadian Arctic Archipelago, and rather cold polar flow over Svalbard and the Barents Sea. This circulation anomaly partly explains the sharply enhanced melt of the Greenland ice sheet (Fettweis et al., 2013; Hanna et al., 2009;

## Recent summer Arctic circulation anomalies in a historical perspective

A. Belleflamme et al.

[Title Page](#)

[Abstract](#)

[Introduction](#)

[Conclusions](#)

[References](#)

[Tables](#)

[Figures](#)

◀

▶

[Back](#)

[Close](#)

[Full Screen / Esc](#)

[Printer-friendly Version](#)

[Interactive Discussion](#)



Rajewicz and Marshall, 2014; Tedesco et al., 2008) and the stabilisation of the melt rate of the Svalbard glaciers (Moholdt et al., 2010) despite Arctic warming (Serreze et al., 2009). Ballinger et al. (2014) highlighted an increase in the summertime frequency of the Beaufort Sea High over the last decade, on the basis of the mean sea level pressure (SLP). They found that this circulation anomaly is significantly anti-correlated with the Arctic Oscillation (AO) index, which has decreased over the same period. Moreover, this anomaly is simultaneous with the increased frequency of the Greenland High described above suggesting that both anomalies are linked. Finally, these circulation anomalies have been pointed (Overland et al., 2012; Wang et al., 2009) to explain the recent Arctic sea ice cover (SIC) decrease (Stroeve et al., 2014). High pressure systems over the Canadian Arctic Archipelago and Greenland favour sea ice export from the Arctic basin through the Fram Strait and the Barents Sea, which is particularly effective for sea ice loss during summer (Wang et al., 2009).

It is interesting to study whether the recent circulation anomalies are unique (and potentially caused by global warming) or if similar anomalies have already occurred during the instrumental period (since the late 19th century) due to the natural variability of the climatic system. We have put the recent (2007–2012) summertime atmospheric circulation anomalies over the Arctic region in perspective with the reconstructed circulation over the instrumental period. To achieve this, we have used an atmospheric circulation type classification (CTC) to individuate the main circulation types over the Arctic region and to analyse their frequency changes over time as done by Ballinger et al. (2014) over the Beaufort Sea and Fettweis et al. (2013) over Greenland. Since the aim of CTCs is to group similar circulation situations together (Huth et al., 2008; Philipp et al., 2010), this methodology allows a synthetic analysis of the atmospheric circulation over a given region at a daily scale (i.e. the characteristic time scale of synoptic circulation patterns like high pressure systems). CTCs are widely used to compare datasets (e.g. reanalyses, global circulation model outputs), to evaluate their ability to reproduce the observed atmospheric circulation, and to detect changes in the observed and projected atmospheric circulation (Anagnostopoulou et al., 2009; Bardossy and Caspary, 1990;

## Recent summer Arctic circulation anomalies in a historical perspective

A. Belleflamme et al.

[Title Page](#)

[Abstract](#)

[Introduction](#)

[Conclusions](#)

[References](#)

[Tables](#)

[Figures](#)

[|◀](#)

[▶|](#)

[◀](#)

[▶](#)

[Back](#)

[Close](#)

[Full Screen / Esc](#)

[Printer-friendly Version](#)

[Interactive Discussion](#)



Belleflamme et al., 2013, 2014; Demuzere et al., 2009; Fettweis et al., 2013; Kyselý and Huth, 2006; Pastor and Casado, 2012; Philipp et al., 2007).

In this study, we apply the CTC developed by Fettweis et al. (2011) (described in Sect. 3) on daily SLP and Z500 fields from different reanalysis datasets (detailed in Sect. 2). In Sect. 4.1.1, we put in perspective the summertime circulation of 2007–2012 with the circulation variability observed since 1871. The influence of the uncertainties of the past circulation on our results is discussed in Sect. 4.1.2. After a comparison between the SLP and the Z500-based results in Sect. 4.2, we analyse the links between the circulation type frequencies and NAO and SIC in Sect. 4.3.

## 10 2 Data

We used daily SLP and Z500 data for the summer months (JJA) of four reanalysis datasets:

- the ERA-Interim reanalysis (Dee et al., 2011) from the European Centre for Medium-Range Weather Forecasts (ECMWF) (spatial resolution:  $0.75^\circ \times 0.75^\circ$ ) over the period 1979–2013,
- the ERA-40 reanalysis from the ECMWF (Uppala et al., 2005) (spatial resolution:  $1.125^\circ \times 1.125^\circ$ ) over the period 1958–1978 as extension for ERA-Interim,
- the NCEP/NCAR reanalysis from the National Centers for Environmental Prediction – National Center for Atmospheric Research (Kalnay et al., 1996) (spatial resolution:  $2.5^\circ \times 2.5^\circ$ ) over the period 1948–2013,
- the Twentieth Century Reanalysis version 2 (20CRv2) (Compo et al., 2011) from the NOAA ESRL/PSD (National Oceanic and Atmospheric Administration Earth System Research Laboratory/Physical Sciences Division) (spatial resolution:  $2^\circ \times 2^\circ$ ) over the period 1871–2012. The 20CRv2 data are constructed as the

[Title Page](#)

[Abstract](#)

[Introduction](#)

[Conclusions](#)

[References](#)

[Tables](#)

[Figures](#)

◀

▶

[Back](#)

[Close](#)

[Full Screen / Esc](#)

[Printer-friendly Version](#)

[Interactive Discussion](#)



ensemble mean of 56 runs. The standard deviation (called spread) of this ensemble mean is also given for each variable (in our case SLP and Z500). We used it to estimate the uncertainty of our 20CRv2-based results, in particular before the overlapping period with the other reanalysis datasets when the assimilated observations are sparse. In fact, the spread, and thus the uncertainty of the reconstructed atmospheric circulation in 20CRv2, strongly depends on the number of available station data, which is low before 1940 (Compo et al., 2011). It is important to note that only SLP is assimilated into 20CRv2 in contrast with other reanalyses where satellite and upper air data are also assimilated every 6 h. Therefore, 20CRv2 is a priori less reliable than the other more constrained reanalyses.

Further, the daily SIC from ERA-Interim is also used over the 1980–2013 JJA period.

Since the reanalyses have different spatial resolutions, and to avoid the problem of decreasing pixel area near the pole when using geographic coordinates, all reanalysis outputs have been linearly interpolated on a regular grid with a spatial resolution of 100 km. Our integration domain is 5000 by 6000 km large and covers the whole Arctic Ocean, Greenland, and the northern part of the Atlantic Ocean (Fig. 1).

Finally, monthly NAO data over the period 1871–2013 were obtained from the Climatic Research Unit (CRU). This NAO index is defined as the normalised difference between the measured SLP on the Azores Isles (Ponta Delgada) and on Iceland (Reykjavik).

### 3 Method

The SLP data from the different reanalyses were compared using the automatic circulation type classification developed by Fettweis et al. (2011) and used over Greenland by Belleflamme et al. (2013) and Fettweis et al. (2013), and over Europe by Belleflamme et al. (2014). This CTC is considered a leader-algorithm method (Philipp et al., 2010), because each class is defined by a reference day and a similarity threshold. A given

<a href="#">Title Page</a>	
<a href="#">Abstract</a>	<a href="#">Introduction</a>
<a href="#">Conclusions</a>	<a href="#">References</a>
<a href="#">Tables</a>	<a href="#">Figures</a>
<a href="#">◀</a>	<a href="#">▶</a>
<a href="#">◀</a>	<a href="#">▶</a>
<a href="#">Back</a>	<a href="#">Close</a>
<a href="#">Full Screen / Esc</a>	
<a href="#">Printer-friendly Version</a>	
<a href="#">Interactive Discussion</a>	

day is assigned to a class if the similarity index between this day and the reference day of the class lies beyond the similarity threshold. The reference day is selected as the day counting the most similar days. The similarity between the days is gauged by the Spearman rank correlation coefficient. The interest of using correlation-based similarity indices is that they are not influenced by the average SLP of a day, but only by its spatial pattern (Philipp et al., 2007). In order to minimize the influence of eventual temperature biases into the SLP retrieving computation, especially over elevated regions like Greenland (Lindsay et al., 2014), we only considered oceanic pixels to perform the SLP-based classification. The same procedure was done using Z500, but all pixels of the domain were taken into account, since there is no more influence of the surface and its elevation at this level.

This CTC is automatic, meaning that the circulation types are built by the algorithm and not predefined by the user. This implies that the circulation types obtained using different datasets will be different and thus difficult to compare. To overcome this problem, we “projected” the types of a reference dataset onto the other datasets, i.e. the types obtained for the reference dataset were imposed as predefined types for the other datasets, as proposed by Huth (2000) and done by Belleflamme et al. (2013) and Belleflamme et al. (2014). Since the types are now the same for all datasets, they can easily be compared. Lindsay et al. (2014) compared seven reanalysis datasets (including ERA-Interim, NCEP/NCAR, and 20CRv2) over the Arctic for the 1980–2009 period and they conclude that ERA-Interim gives the best results for various variables (e.g. SLP, T2M, wind speed) compared with observations. Thus, we used the ERA-Interim dataset over the 1980–2012 period, which is common to all reanalyses, as reference dataset.

As said above, the 20CRv2 reanalysis SLP data are given as an ensemble mean of 56 runs and the spread around this ensemble mean. To evaluate the uncertainty from the 20CRv2-based data estimated by this spread, we have performed 20 000 classification runs. For each run, the daily spread, multiplied by a factor varying randomly between –1 and 1, is added to the daily SLP. Due to the high number of runs, all

## Recent summer Arctic circulation anomalies in a historical perspective

A. Belleflamme et al.

[Title Page](#)

[Abstract](#)

[Introduction](#)

[Conclusions](#)

[References](#)

[Tables](#)

[Figures](#)

[|◀](#)

[▶|](#)

[◀](#)

[▶](#)

[Back](#)

[Close](#)

[Full Screen / Esc](#)

[Printer-friendly Version](#)

[Interactive Discussion](#)



## Recent summer Arctic circulation anomalies in a historical perspective

A. Belleflamme et al.

[Title Page](#)

[Abstract](#)

[Introduction](#)

[Conclusions](#)

[References](#)

[Tables](#)

[Figures](#)

[|◀](#)

[▶|](#)

[◀](#)

[▶](#)

[Back](#)

[Close](#)

[Full Screen / Esc](#)

[Printer-friendly Version](#)

[Interactive Discussion](#)

multiplying factor values have equal likelihood and their average tends to zero. Thus, no systematic SLP bias is introduced in the 20 000-run ensemble. If adding or subtracting the spread implies a sufficient alteration in the SLP pattern of a given day, this day could be classified into another circulation type, compared to the run using the 20CRv2 SLP ensemble mean (called hereafter 20CRv2 reference run). The same procedure has been done for Z500.

In our CTC, the number of classes is fixed by the user. On the basis of the ERA-Interim SLP over the 1980–2012 summers (JJA), six circulation types were retained in order to obtain the two patterns in which we are the most interested in, i.e. the Beaufort Sea High and the Greenland High. In addition, minimizing the number of types allows a more concise and synthetic analysis. The six obtained circulation types can be described as follows (Fig. 1): Type 1 is characterised by a low pressure system centred over the Arctic Ocean and represents about 14 % of the classified days over 1980–2012. On the opposite, Type 2 is marked by a high pressure located over the Beaufort Sea and the western part of the Arctic Ocean. Type 3 presents a strong Icelandic low and higher pressure along the Russian coast. Type 4 is the Greenland High type and accounts for 24 % of the classified days. Types 5 and 6 show opposite patterns, with a low (resp. high) pressure east of Svalbard surrounded by high (resp. low) pressure systems. It is important to note that Type 6 also contains the unclassified days, i.e. the days that are too different from the other types (< 1 % of the classified days for the ERA-Interim reference classification).

Despite that the SLP and Z500-based circulation types are different, six types were also retained for Z500 (Supplement Fig. S1). Type 1 is characterised by a strong depression centred over the Arctic Ocean. This depression is located more eastward in Type 2, which also presents a slight ridge over Greenland. In Type 3, the depression is situated over the Greenland and Svalbard region. Type 4 is marked by two depressions, the Icelandic Low and a low over the Chukchi Sea, and a ridge over the Barents and Kara Seas. Type 5 combines the Greenland High and the Beaufort Sea High. Finally, Type 6 shows a high pressure system over the Arctic Ocean, while the depression is

split into three parts (i.e. the Icelandic Low, a low over the Kara Sea, and a low over the Canadian Arctic Archipelago).

## 4 Results

There is a very good agreement between the frequencies of the circulation types and their evolution over time for all reanalyses over 1958–2012, as well for SLP (Fig. 2) as for Z500 (Supplement Fig. S2). The only notable difference is a systematic overestimation of about 4–6 % of the frequency of Type 3 to the detriment of Type 2 by 20CRv2 compared to the full constrained reanalyses (ERA and NCEP/NCAR) for SLP. This bias is in agreement with the findings of Lindsay et al. (2014), who report a positive SLP bias over Asia for 20CRv2 (using monthly data), since Type 3 is characterised by an anticyclone over the Asian part of the domain, in contrary to Type 2.

### 4.1 Sea level pressure

#### 4.1.1 Circulation type frequency evolution

The frequencies of Type 2 (Beaufort Sea – Arctic Ocean High) and of Type 4 (Greenland High) have almost doubled over 2007–2012 compared to the 1871–2013 average (Fig. 2). These frequency anomalies join the findings of Ballinger et al. (2014) for the Beaufort Sea and Fettweis et al. (2013) for Greenland. They are compensated by a decrease in frequency of Type 3 by a factor of two, and to a lesser extent of Type 1. Both types are characterised by a low pressure system over the Arctic. Types 2 and 4 both never experienced such high frequencies over several consecutive summers since 1871. Between 2007 and 2012, two summers for Type 2 and five summers for Type 4 presented a higher frequency than the 90th percentile frequency, meaning a return period of about 10 years (Table 1). However, 20CRv2 suggests that similar circulation type frequencies were observed before 1880 while the uncertainty is very high over that period. Another period with similar atmospheric circulation conditions is observed around

[Title Page](#)

[Abstract](#)

[Introduction](#)

[Conclusions](#)

[References](#)

[Tables](#)

[Figures](#)

◀

▶

[Back](#)

[Close](#)

[Full Screen / Esc](#)

[Printer-friendly Version](#)

[Interactive Discussion](#)

1957–1960. Finally, Type 4 shows some summers with anomalously high frequencies between 1891 and 1896. Nevertheless, these three periods were shorter than 2007–2012 and not marked by as many anomalous summers, except for the 1891–1896 period for Type 4. The anomalies of the frequencies of Types 2 and 4 (+20 %), and 5 Type 3 (−15 to −20 %), are much higher than their interannual frequency variability (with a standard deviation over the 1871–2012 period for the 20CRv2 20 000-run ensemble mean of about 7.7 %, 9.7 %, and 8.2 % for Types 2, 3, and 4 respectively). The frequency anomalies of the other types are of the same order than their interannual variability (with a standard deviation of about 9.4 %, 5 %, and 5.6 % for Types 1, 5, 10 and 6 respectively). Wu et al. (2014) showed that the progressive intensification of the Beaufort Sea High over 1979–2005 can only be reproduced by climate models by including the observed greenhouse gas concentration increase. This could suggest that the 2007–2012 frequency anomalies are related to global warming. However, the 2013 summer shows opposite extremes. This suggests that, even if the 2007–2012 circulation 15 anomalies might be related to global warming, this link is not straightforward, and the natural variability could largely exceed the global warming induced signal.

The circulation type frequency anomalies are not due to changes in the persistence (i.e. the duration of consecutive days grouped in the same type). In fact, there is a persistence increase for Types 2 and 4, and a decrease for Type 3 over 2007–2012 with 20 regard to the overall average (not shown). But a more detailed analysis shows that these persistence changes are artefacts due to the frequency anomalies. Note that the 20CRv2 20 000-run ensemble persistence cannot be used for a persistence analysis. Since the spread is added with a multiplying factor determined randomly for each day, the continuity of the atmospheric circulation over time, i.e. the transitions between the 25 circulation types and the succession of the types themselves, is not preserved.

The analysis of the 20CRv2 reference run monthly circulation type frequencies shows that the 2007–2012 frequency anomalies affect all three months (JJA). In this way, the 2007–2012 period differs from the other anomalous periods (1871–1880, 1891–1896, and 1957–1960). For example, the positive frequency anomaly of Type

<a href="#">Title Page</a>	
<a href="#">Abstract</a>	<a href="#">Introduction</a>
<a href="#">Conclusions</a>	<a href="#">References</a>
<a href="#">Tables</a>	<a href="#">Figures</a>
<a href="#">◀</a>	<a href="#">▶</a>
<a href="#">◀</a>	<a href="#">▶</a>
<a href="#">Back</a>	<a href="#">Close</a>
<a href="#">Full Screen / Esc</a>	
<a href="#">Printer-friendly Version</a>	
<a href="#">Interactive Discussion</a>	

2 over 1958–1960 is due to high frequencies during August and to a lesser extent during June. For the year 1957, Type 4 shows frequencies far above normal for June and July, but not for August. The 1871–1880 period has many summers with above normal frequencies for Type 4, but no systematic frequency anomaly lasting a few summers can be detected for one particular month.

#### 4.1.2 20CRv2 frequency uncertainty

The uncertainty of the 20CRv2 frequencies strongly decreases between 1930 and 1950 to become insignificant over the four or five last decades for all types (Fig. 2). It is interesting to observe that this uncertainty remains relatively constant over time before 1940, turning around 7–11 % for the first four types, and around 4–6 % for Types 5 and 6. Moreover, the 20 000-run ensemble mean frequency, its standard deviation, and its 10th and 90th percentiles show an evolution over time that is almost parallel to the 20CRv2 reference run. There is no smoothing of the interannual variability, which remains similar to the variability of the last decades when going back in time. Finally, the last class, which groups the unclassified days, does not show any increase towards the beginning of the 20CRv2 period, meaning that there are not more days that do not correspond to the main types before 1940 than over the three last decades (1980–2012). Thus, even if there is some uncertainty about the exact frequencies before 1940, there is high confidence in the magnitude and the time evolution of the circulation type frequencies.

There are significant circulation type frequency differences between the 20 000-run ensemble mean and the 20CRv2 reference run before 1940. In particular, the frequency of Types 1 and 2 is strongly overestimated by the 20 000-run ensemble compared to the 20CRv2 reference run. The 20CRv2 reference run annual frequencies turn around the 10th percentile of the 20 000-run ensemble for these two types. This is compensated by an underestimation of the frequencies of the other types by the 20 000-run ensemble whose 90th percentile frequencies are of the same order than the 20CRv2 reference run frequencies. These frequency shifts are due to the pattern of the SLP

<a href="#">Title Page</a>	
<a href="#">Abstract</a>	<a href="#">Introduction</a>
<a href="#">Conclusions</a>	<a href="#">References</a>
<a href="#">Tables</a>	<a href="#">Figures</a>
<a href="#">◀</a>	<a href="#">▶</a>
<a href="#">◀</a>	<a href="#">▶</a>
<a href="#">Back</a>	<a href="#">Close</a>
<a href="#">Full Screen / Esc</a>	
<a href="#">Printer-friendly Version</a>	
<a href="#">Interactive Discussion</a>	

- spread, which is much higher over the Arctic Ocean than over the rest of the domain for the 1871–1930 period (Fig. 3, bottom). Consequently, when adding (with a multiplying factor between 0 and 1) the SLP spread, the pattern of the SLP daily mean is changed towards a more anticyclonic pattern over the Arctic Ocean, making it similar to 5 Type 2. In the same way, when subtracting (with a multiplying factor between –1 and 0) the SLP spread, the SLP daily mean becomes more similar to Type 1, which presents a low pressure over the Arctic Ocean. Further, since the Spearman rank correlation coefficient is not sensitive to the average SLP, but only to the SLP pattern, the evolution of the frequency uncertainty over time is rather related to the spatial maximum and the 10 standard deviation of the SLP spread than to its average, which decreases as soon as the beginning of the 20CRv2 era (Fig. 3, top).

## 4.2 Geopotential height at 500 hPa

- The detected frequency changes are similar to those of SLP. The Greenland High and the Beaufort Sea High (Types 2 and 5) were almost twice as frequent over 2007–2012 15 than over the whole 1871–2013 period (Supplement Fig. S2, Table S1). For Type 2 (Greenland High), two of the three other high frequency periods found for SLP are also detected: 1871–1880 and 1891–1896. The 1957–1960 period is not exceptional on the basis of Z500.

- As for SLP, the Z500 spread plays an important role in the frequency distribution 20 before 1940, when it is the highest (Supplement Fig. S3, top). Before 1940, the frequencies of the 20CRv2 reference run and to a lesser extent of the 20 000-run ensemble mean are much higher for Type 1 (about 20 %) and Type 2 (about 10 %) with respect to the second half of the 20th century. This is compensated by particularly low 25 frequencies of Types 3, 5, and 6, and to a lesser extent of Type 4. These frequency shifts are probably due to the uncertainties in the 20CRv2 data before 1940 since they are lower for the 20 000-run ensemble compared to the 20CRv2 reference run. Moreover, as for SLP, the frequency differences between the 20CRv2 reference run and the 20 000-run ensemble mean can be explained by the pattern of the Z500 spread, which

[Title Page](#)[Abstract](#)[Introduction](#)[Conclusions](#)[References](#)[Tables](#)[Figures](#)[|◀](#)[▶|](#)[◀](#)[▶](#)[Back](#)[Close](#)[Full Screen / Esc](#)[Printer-friendly Version](#)[Interactive Discussion](#)

is very close to the SLP spread pattern (Supplement Fig. S3, bottom). When subtracting the spread, the circulation tends to become more cyclonic over the Arctic Ocean, favouring the shift of days into Types 1, 2, and 4. In the same way, adding the spread gives a more anticyclonic character to the circulation. This favours Types 3, 5, and 6.

5 But Types 1 and 2 count for about 80 % of all days before 1940. Therefore, adding the spread to the detriment of these types has much more impact on the frequency distribution than subtracting the spread, since most days will remain in their original class.

### 4.3 Links with other variables

#### 10 4.3.1 North Atlantic Oscillation

The 30 year running correlation between the circulation type frequencies and the JJA CRU NAO index (calculated as the average of the JJA monthly CRU NAO index values) shows a very good agreement between the different reanalyses on the basis of SLP and Z500. Further, the almost similar evolution of this correlation for the 20CRv2 reference run and the 20 000-run ensemble mean confirms that taking into account the spread does not impact the frequency variations over time.

15 For the SLP-based classification, Types 2 and 4 both show negative correlations with NAO, while only the correlation of Type 3 is always positive (Fig. 4). The link between NAO and the three other types is not as clear. The association of negative NAO phases with high frequencies for Types 2 and 4, which is even more evident when adding both frequencies together, becomes more marked when the 2007–2012 anomalous summers are integrated into the calculations (i.e. starting in 1992), suggesting a stronger link over that period. This is in agreement with Fettweis et al. (2013), who linked the recent circulation anomalies and the negative NAO anomalies. For the three other periods with circulation anomalies (1871–1880, 1891–1896, and 1957–1960), there is no clear link between NAO, which is less exceptional than over 2007–2012, and the frequency of Types 2 and 4.

[Title Page](#)[Abstract](#)[Introduction](#)[Conclusions](#)[References](#)[Tables](#)[Figures](#)[◀](#)[▶](#)[◀](#)[▶](#)[Back](#)[Close](#)[Full Screen / Esc](#)[Printer-friendly Version](#)[Interactive Discussion](#)

The Z500-based results are basically the same as for SLP. Type 2 shows a negative correlation, while the correlation between NAO and the frequency of Type 1 is always positive (Supplement Fig. S4). Nevertheless, the correlation of Type 5 is not as clear.

While it is negative since 1960, the 20CRv2 reference run and the 20 000-run ensemble mean show divergent values before 1940 suggesting that the uncertainty due to the 20CRv2 spread has more impact on our results for Z500 than for SLP. This is certainly reinforced by the underestimation of the frequency of Type 5 before 1940. Again, the link between NAO and Types 2 and 5 is stronger over 2007–2012, compared to 1871–2013.

### 10 4.3.2 Sea ice cover

There is a link between the circulation anomalies and the summertime sea ice cover (SIC) loss. As indicated by the correlation between the ERA-Interim SIC loss and the ERA-Interim SLP-based circulation type frequencies over 1980–2013, SIC loss is only favoured by Types 2 ( $r = -0.53$ ) and 4 ( $r = -0.50$ ), while Types 1 ( $r = 0.52$ ) and 3 ( $r = 0.52$ ) tend to mitigate it. Types 5 ( $r = 0.22$ ) and 6 ( $r = 0.14$ ) do not have important impacts on the SIC loss. When considering the sum of the frequencies of Types 2 and 4, the relation appears to be even clearer with a correlation of  $-0.68$ . This means that the frequency increase of Types 2 and 4 could partly explain the summertime record Arctic SIC loss observed over the last decade.

For the Z500-based classification, only Type 5 ( $r = -0.66$ ) can be clearly related to enhanced SIC loss and Type 1 ( $r = 0.62$ ) to mitigated SIC loss. For the remaining types, the correlation varies between  $-0.18$  and  $0.05$ . As said above, Type 5 combines the Beaufort Sea High and the Greenland High. Type 2 shows only a slight ridge over Greenland and a depression centred over the Arctic Ocean, far away from the Russian coast. Thus, the conditions favouring sea ice export through the Fram Strait and the Barents Sea are not met for this type, as confirmed by its poor correlation ( $r = -0.18$ ) with SIC.

[Title Page](#)[Abstract](#)[Introduction](#)[Conclusions](#)[References](#)[Tables](#)[Figures](#)[|◀](#)[▶|](#)[◀](#)[▶](#)[Back](#)[Close](#)[Full Screen / Esc](#)[Printer-friendly Version](#)[Interactive Discussion](#)

Our results seem to confirm those of Wang et al. (2009) and Overland et al. (2012), who showed that summers characterised by a higher occurrence of a high pressure system over the Canadian Arctic Archipelago and Greenland and a low pressure system over the Kara and Laptev Seas are marked by enhanced SIC loss.

## 5 Conclusions

We used an automatic circulation type classification to study the anomalies in the summertime (JJA) atmospheric circulation based on (i) the sea level pressure and (ii) the 500 hPa geopotential height over the Arctic region over the 1871–2013 period. Three reanalysis datasets were used over the second half of the 20th century (ERA-Interim as reference, ERA-40, and NCEP/NCAR). The 20CRv2 reanalysis was used over the 1871–2012 period to evaluate if circulation anomalies similar to 2007–2012 could already have occurred. Further, since 20CRv2 data are given as a 56-member ensemble mean with its standard deviation (spread), 20 000 runs have been done to take into account the 20CRv2 uncertainty. For these runs, the spread multiplied by a factor varying randomly between –1 and 1 has been added to the daily mean.

Despite an uncertainty of about 5 to 11 % for the circulation type frequencies before 1930, the magnitude and the time evolution of the frequency anomalies can be reasonably well estimated using 20CRv2 SLP. Further, this uncertainty becomes less significant after 1950, due to improved assimilated data availability and reliability. The particular spatial pattern of the spread, i.e. highest over the Arctic Ocean, causes a strong overestimation of Type 1 (low pressure over the Arctic Ocean) and Type 2 (high pressure over the Arctic Ocean) to the detriment of all other types for the SLP-based 20 000-run ensemble compared to the 20CRv2 reference run. Thus, it is interesting to note that, although no systematic SLP bias is introduced through adding the spread, systematic circulation type frequency shifts appear. In a similar way, the Z500 spread also introduces artefacts in the 20 000-run ensemble. This shows the necessity

TCD

8, 4823–4847, 2014

## Recent summer Arctic circulation anomalies in a historical perspective

A. Belleflamme et al.

<a href="#">Title Page</a>	
<a href="#">Abstract</a>	<a href="#">Introduction</a>
<a href="#">Conclusions</a>	<a href="#">References</a>
<a href="#">Tables</a>	<a href="#">Figures</a>
<a href="#">◀</a>	<a href="#">▶</a>
<a href="#">◀</a>	<a href="#">▶</a>
<a href="#">Back</a>	<a href="#">Close</a>
<a href="#">Full Screen / Esc</a>	
<a href="#">Printer-friendly Version</a>	
<a href="#">Interactive Discussion</a>	

## Recent summer Arctic circulation anomalies in a historical perspective

A. Belleflamme et al.

[Title Page](#)

[Abstract](#)

[Introduction](#)

[Conclusions](#)

[References](#)

[Tables](#)

[Figures](#)

[|◀](#)

[▶|](#)

[◀](#)

[▶](#)

[Back](#)

[Close](#)

[Full Screen / Esc](#)

[Printer-friendly Version](#)

[Interactive Discussion](#)

to take into account the spread of the 20CRv2 data to get an estimation of the range of plausible results.

We have found the same summertime circulation anomalies as described by other authors (Ballinger et al., 2014; Fettweis et al., 2013), i.e. a doubling in frequency of the Beaufort Sea – Arctic Ocean High and of the Greenland High over 2007–2012. Only three other periods (1871–1880, 1891–1896, and 1957–1960) of similar circulation anomalies were detected but the successions of summers with such anomalies are shorter than in the 2000's. These pointed anomalies largely exceed the interannual variability of the circulation type frequencies. Nevertheless, it is not possible to attribute the circulation anomalies over 2007–2012 to global warming. First, these anomalies are observed over a too short period, so that they could be an exceptionally strong deviance from the average circulation. In this way, the 2013 summer was marked by opposite frequency extremes, positive NAO index values, a low melt of the Greenland ice sheet, and lower Arctic sea ice decline compared to 2007–2012. Our findings corroborate those of Rajewicz and Marshall (2014), who state that the 2013 JJA mean Z500 over Greenland was significantly lower than the average over the last seven decades, which contrasts with the strong positive anomaly of the preceding summers. Secondly, as said above, similar circulation conditions were observed before 1880 and around 1891–1896, when the Arctic climate was likely much colder than now.

Our findings confirm those of Ballinger et al. (2014) and Overland et al. (2012), who detected that the Beaufort Sea High is associated with anticyclonic conditions over Greenland. This is particularly clear for the Z500-based classification, where Type 5 combines both the Beaufort Sea High and the Greenland High. Moreover, the circulation type frequency anomalies observed over the 2007–2012 period on the basis of SLP and Z500 are linked with the measured negative NAO trend. Thus, our results seem to be in agreement with the hypothesis of Overland et al. (2012), who suggest that the Beaufort Sea High and the Greenland High frequency increases might be part of an enhanced North-American blocking mechanism.

The observed summertime decrease in sea ice cover (SIC) between 1980 and 2013 seems to be partly due to the higher occurrence of the Beaufort Sea High and the Greenland High. This means that, in addition to the factors influencing the Arctic sea ice melt cited by Stroeve et al. (2014) (e.g. generalised warming over the Arctic, earlier 5 melt onset, enhanced ice-albedo feedback, increased sea surface temperature, and a delayed autumn freeze up), the JJA atmospheric circulation could also play a significant role in the sea ice melt. However, some studies (e.g. Inoue et al., 2012; Petoukhov and Semenov, 2010) suggest that atmospheric circulation changes can be induced by 10 SIC anomalies. Therefore, the recent SIC decrease could be a trigger of the recent atmospheric circulation change inducing in turn a SIC decrease, suggesting a positive feedback.

**The Supplement related to this article is available online at  
doi:10.5194/tcd-8-4823-2014-supplement.**

*Acknowledgements.* NCEP/NCAR reanalysis data were provided by the NOAA/OAR/ESRL PSD, Boulder, Colorado, USA, from their website at <http://www.esrl.noaa.gov/psd/>.

The ECMWF ERA-40 and ERA-Interim reanalysis data used in this study were obtained from the ECMWF Data Server (<http://www.ecmwf.int>).

Support for the Twentieth Century Reanalysis (20CR) Project dataset was provided by the US Department of Energy, Office of Science Innovative and Novel Computational Impact on 20 Theory and Experiment (DOE INCITE) program, by the Office of Biological and Environmental Research (BER), and by the National Oceanic and Atmospheric Administration (NOAA) Climate Program Office ([http://www.esrl.noaa.gov/psd/data/gridded/data.20thC\\_ReanV2.html](http://www.esrl.noaa.gov/psd/data/gridded/data.20thC_ReanV2.html)).

The monthly NAO data were obtained from the University of East Anglia (UEA) Climatic Research Unit (CRU) website (<http://www.cru.uea.ac.uk/cru/data/nao/>).

## Recent summer Arctic circulation anomalies in a historical perspective

A. Belleflamme et al.

[Title Page](#)

[Abstract](#)

[Introduction](#)

[Conclusions](#)

[References](#)

[Tables](#)

[Figures](#)

[|◀](#)

[▶|](#)

[◀](#)

[▶](#)

[Back](#)

[Close](#)

[Full Screen / Esc](#)

[Printer-friendly Version](#)

[Interactive Discussion](#)



## References

## Recent summer Arctic circulation anomalies in a historical perspective

A. Belleflamme et al.

Title Page

Abstract

Introduction

Conclusions

References

Tables

Figures

◀

▶

◀

▶

Back

Close

Full Screen / Esc

Printer-friendly Version

Interactive Discussion



## Recent summer Arctic circulation anomalies in a historical perspective

A. Belleflamme et al.

- Fettweis, X., Mabille, G., Erpicum, M., Nicolay, S., and Van den Broeke, M.: The 1958–2009 Greenland ice sheet surface melt and the mid-tropospheric atmospheric circulation, *Clim. Dynam.*, 36, 139–159, doi:10.1007/s00382-010-0772-8, 2011. 4826, 4827
- Fettweis, X., Hanna, E., Lang, C., Belleflamme, A., Erpicum, M., and Gallée, H.: *Brief communication* "Important role of the mid-tropospheric atmospheric circulation in the recent surface melt increase over the Greenland ice sheet", *The Cryosphere*, 7, 241–248, doi:10.5194/tc-7-241-2013, 2013. 4824, 4825, 4826, 4827, 4830, 4834, 4837
- Hanna, E., Cappelen, J., Fettweis, X., Huybrechts, P., Luckman, A., and Ribergaard, M. H.: Hydrologic response of the Greenland ice sheet: the role of oceanographic warming, *Hydrol. Process.* (Special issue: Hydrol. Effect Shrink Cryosphere), 23, 7–30, doi:10.1002/hyp.7090, 2009. 4824
- Huth, R.: A circulation classification scheme applicable in GCM studies, *Theor. Appl. Climatol.*, 67, 1–18, doi:10.1007/s007040070012, 2000. 4828
- Huth, R., Beck, C., Philipp, A., Demuzere, M., Ustrnul, Z., Cahynová, M., Kyselý, J., and Tveito, O. E.: Classifications of atmospheric circulation patterns: Recent advances and applications, *Ann. NY. Acad. Sci.*, 1146, 105–152, doi:10.1196/annals.1446.019, 2008. 4825
- Inoue, J., Hori, M., and Takaya, K.: The role of Barents sea ice in the wintertime cyclone track and emergence of a warm-Arctic cold-Siberian Anomaly, *J. Climate.*, 25, 2561–2568, doi:10.1175/JCLI-D-11-00449.1, 2012. 4838
- Kalnay, E., Kanamitsu, M., Kistler, R., Collins, W., Deaven, D., Gandin, L., Iredell, M., Saha, S., White, G., Woollen, J., Zhu, Y., Leetmaa, A., Reynolds, B., Chelliah, M., Ebisuzaki, W., Higgins, W., Janowiak, J., Mo, K., Ropelewski, C., Wang, J., Jenne, R., and Joseph, D.: The NCEP/NCAR 40-Year Reanalysis Project, *B. Am. Meteorol. Soc.*, 77, 437–471, doi:10.1175/1520-0477(1996)077<0437:TNYRP>2.0.CO;2, 1996. 4826
- Kyselý, J. and Huth, R.: Changes in atmospheric circulation over Europe detected by objective and subjective methods, *Theor. Appl. Climatol.*, 85, 19–36, doi:10.1007/s00704-005-0164-x, 2006. 4826
- Lindsay, R., Wensnahan, M., Schweiger, A., and Zhang, J.: Evaluation of seven different atmospheric reanalysis products in the Arctic, *J. Climate.*, 27, 2588–2606, doi:10.1175/JCLI-D-13-00014.1, 2014. 4828, 4830
- Moholdt, G., Nuth, C., Hagen, J., and Köhler, J.: Recent elevation changes of Svalbard glaciers derived from ICE-Sat laser altimetry, *Remote. Sens. Environ.*, 114, 2756–2767, doi:10.1016/j.rse.2010.06.008, 2010. 4825

Discussion Paper | Discussion Paper

[Title Page](#)

[Abstract](#)

[Introduction](#)

[Conclusions](#)

[References](#)

[Tables](#)

[Figures](#)

[◀](#)

[▶](#)

[Back](#)

[Close](#)

[Full Screen / Esc](#)

[Printer-friendly Version](#)

[Interactive Discussion](#)



## Recent summer Arctic circulation anomalies in a historical perspective

A. Belleflamme et al.

- Overland, J., Francis, J., Hanna, E., and Wang, M.: The recent shift in early summer Arctic atmospheric circulation, *Geophys. Res. Lett.*, 39, L19804, doi:10.1029/2012GL053268, 2012. 4825, 4836, 4837
- Pastor, M. and Casado, M.: Use of circulation types classifications to evaluate AR4 climate models over the Euro-Atlantic region, *Clim. Dynam.*, 39, 2059–2077, doi:10.1007/s00382-012-1449-2, 2012. 4826
- Petoukhov, V. and Semenov, V.: A link between reduced Barents-Kara sea ice and cold winter extremes over northern continents, *J. Geophys. Res.*, 115, D21111, doi:10.1029/2009JD013568, 2010. 4838
- Philipp, A., Della-Marta, P., Jacobbeit, J., Fereday, D., Jones, P., Moberg, A., and Wanner, H.: Long-term variability of daily North Atlantic-European pressure patterns since 1850 classified by simulated annealing clustering, *J. Climate.*, 20, 4065–4095, doi:10.1175/JCLI4175.1, 2007. 4826, 4828
- Philipp, A., Bartholy, J., Beck, C., Erpicum, M., Esteban, P., Fettweis, X., Huth, R., James, P., Jourdain, S., Kreienkamp, F., Krennert, T., Lykoudis, S., Michalides, S., Pianko, K., Post, P., Rassilla Álvarez, D., Schiemann, R., Spekat, A., and Tymvios, F. S.: COST733CAT – a database of weather and circulation type classifications, *Phys. Chem. Earth*, 35, 360–373, doi:10.1016/j.pce.2009.12.010, 2010. 4825, 4827
- Rajewicz, J. and Marshall, S.: Variability and trends in anticyclonic circulation over the Greenland ice sheet, 1948–2013, *Geophys. Res. Lett.*, 41, 2842–2850, doi:10.1002/2014GL059255, 2014. 4825, 4837
- Serreze, M. C., Barrett, A. P., Stroeve, J. C., Kindig, D. N., and Holland, M. M.: The emergence of surface-based Arctic amplification, *The Cryosphere*, 3, 11–19, doi:10.5194/tc-3-11-2009, 2009. 4825
- Stroeve, J., Markus, T., Boisvert, L., Miller, J., and Barrett, A.: Changes in Arctic melt season and implications for sea ice loss, *Geophys. Res. Lett.*, 41, 1216–1225, doi:10.1002/2013GL058951, 2014. 4825, 4838
- Tedesco, M., Serreze, M., and Fettweis, X.: Diagnosing the extreme surface melt event over southwestern Greenland in 2007, *The Cryosphere*, 2, 159–166, doi:10.5194/tc-2-159-2008, 2008. 4825
- Uppala, S. M., Källberg P. W., Simmons, A. J., Andrae, U., da Costa Bechtold, V., Fiorino, M., Gibson, J. K., Haseler, J., Hernandez, A., Kelly, G. A., Li, X., Onogi, K., Saarenrinne, S., Sokka, N., Allan, R. P., Andersson, E., Arpe, K., Balmaseda, M. A., Bel-

[Title Page](#)

[Abstract](#) [Introduction](#)

[Conclusions](#) [References](#)

[Tables](#) [Figures](#)

◀

▶

◀

▶

[Back](#) [Close](#)

[Full Screen / Esc](#)

[Printer-friendly Version](#)

[Interactive Discussion](#)



- jaars, A. C. M., van de Berg, L., Bidlot, J., Bormann, N., Caires, S., Chevallier, F., De-thof, A., Dragosavac, M., Fisher, M., Fuentes, M., Hagemann, S., Hólm, E., Hoskins, B., Isaksen, L., Janssen, P. A. E. M., Jenne, R., McNally, A. P., Mahfouf, J.-F., Morcrette, J.-J., Rayner, N. A., Saunders, R. W., Simon, P., Sterl, A., Trenberth, K. E., Untch, A., Vasiljevic, D., Viterbo, P., and Woollen, J.: The ECMWF re-analysis, *Q. J. Roy. Meteor. Soc.*, 131, 2961–3012, doi:10.1256/qj.04.176, 2005. 4826
- Wang, J., Zhang, J., Watanabe, E., Ikeda, M., Mizobata, K., Walsh, J., Bai, X., and Wu, B.: Is the Dipole Anomaly a major driver to record lows in Arctic summer sea ice extent? *Geophys. Res. Lett.*, 36, L05706, doi:10.1029/2008GL036706, 2009. 4825, 4836
- Wu, Q., Zhang, J., Zhang, X., and Tao, W.: Interannual variability and long-term changes of atmospheric circulation over the Chukchi and Beaufort Seas, *J. Climate.*, 27, 4871–4889, doi:10.1175/JCLI-D-13-00610.1, 2014. 4831

## Recent summer Arctic circulation anomalies in a historical perspective

A. Belleflamme et al.

[Title Page](#)

[Abstract](#)

[Introduction](#)

[Conclusions](#)

[References](#)

[Tables](#)

[Figures](#)

[|◀](#)

[▶|](#)

[◀](#)

[▶](#)

[Back](#)

[Close](#)

[Full Screen / Esc](#)

[Printer-friendly Version](#)

[Interactive Discussion](#)



**Table 1.** For the SLP-based circulation types, which show a frequency increase over the 2007–2012 period, the summers presenting a higher frequency than the 90th percentile frequency (i.e. a 10 year return period) on the basis of the 20CRv2 reference run over 1871–2012 (JJA) are listed chronologically.

Type 2	Type 4
1873	1871
1877	1872
1879	1880
1891	1928
1897	1957
1911	1958
1912	1971
1923	1977
1948	1980
1960	1993
1965	2007
1982	2008
1987	2009
2007	2011
2011	2012

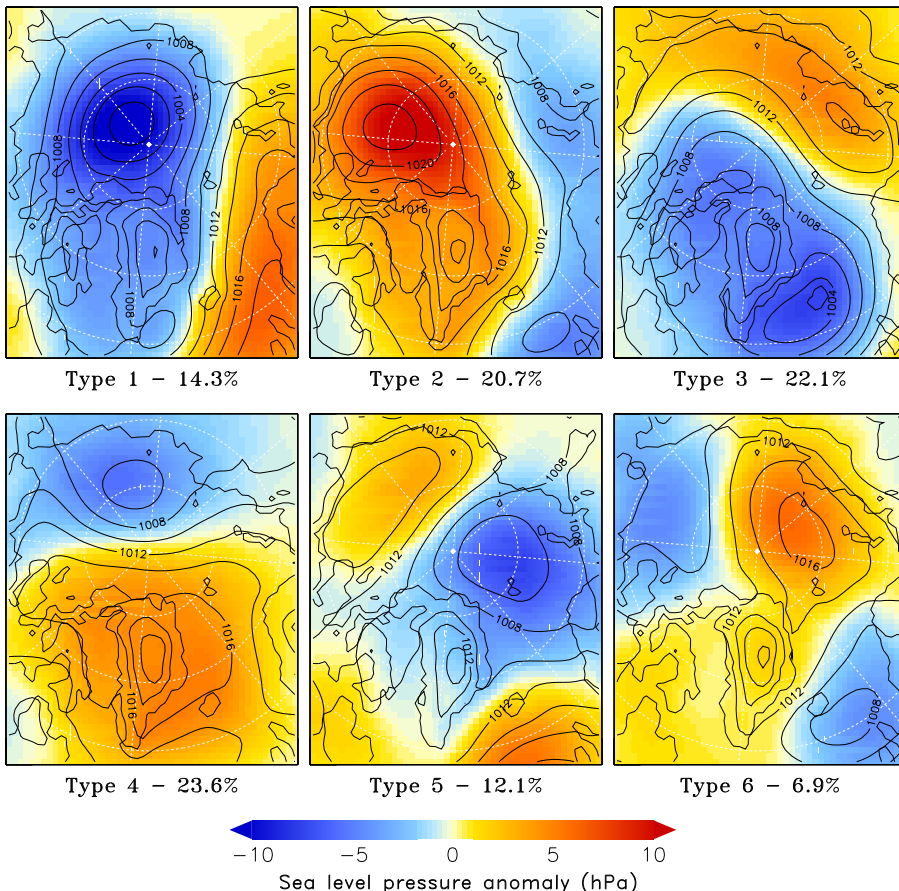


**Figure 1.** The SLP-based reference circulation types over the 1980–2012 (JJA) period for ERA-Interim are represented by the solid black isobars (in hPa). The SLP anomaly (in colours) is calculated as the difference between the class mean SLP and the seasonal mean SLP over 1980–2012. The average frequency of each type is also given.

4844

# Recent summer Arctic circulation anomalies in a historical perspective

A. Belleflamme et al.

Title Page

## Abstract

## Introduction

## Conclusions

## References

Tables

## Figures

1

1

Back

Close

Full Screen / Esc

[Printer-friendly Version](#)

## Interactive Discussion



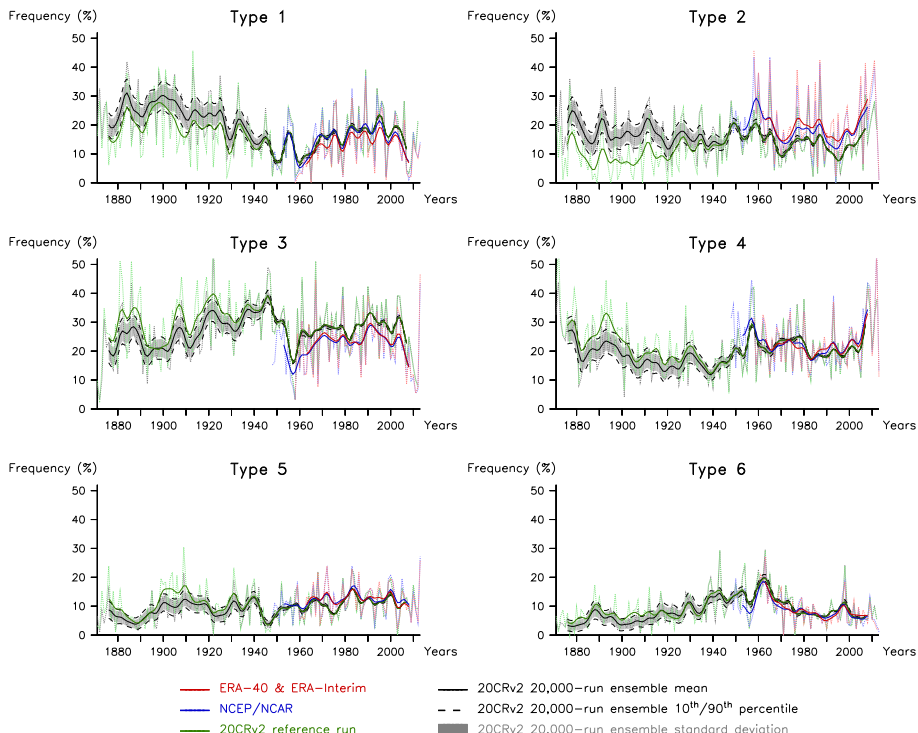


**Figure 2.** The solid lines are calculated as the 10 year binomial running mean frequencies and the dotted light lines are the corresponding annual (JJA) SLP-based frequencies.

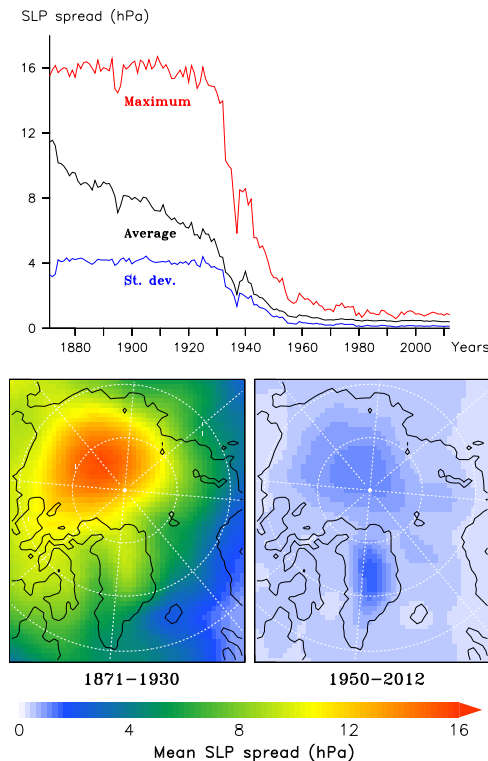


**Figure 3.** Top: the average SLP spread and its standard deviation are calculated as the seasonal (JJA) average 20CRv2 spread and its standard deviation over the oceanic pixels of our domain. The maximum SLP spread is the value of the oceanic pixel showing the highest seasonal (JJA) average spread of each year. Bottom: the SLP spread is calculated as the average 20CRv2 spread over the 1871–1930 summers (JJA), left, and over the 1950–2012 summers, right.

## Recent summer Arctic circulation anomalies in a historical perspective

A. Belleflamme et al.

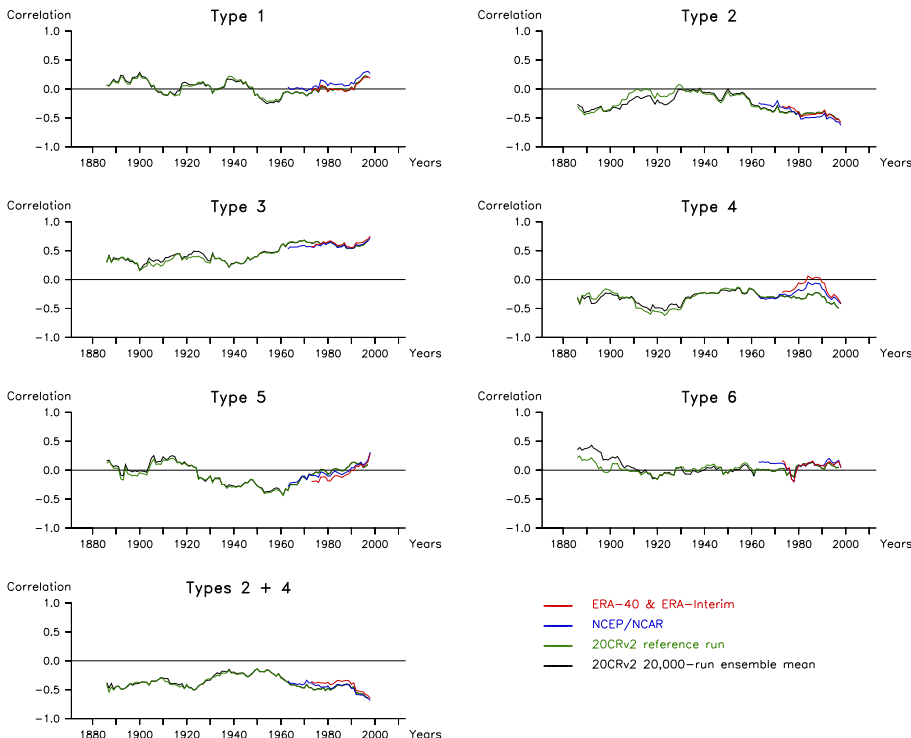


**Figure 4.** The 30 year running correlation is calculated between the annual (JJA) SLP-based frequencies of each type and the JJA CRU NAO index. For the “Types 2 + 4” correlation, the frequencies of Types 2 and 4 have been summed before computing the correlation.